Akademie věd České republiky

Teze disertace
k získání vědeckého titulu "doktor věd"
ve skupině věd: TECHNICKÉ VĚDY

# ULTRAFAST ALL-OPTICAL SIGNAL PROCESSING

……
název disertace

Komise pro obhajoby doktorských disertací v oboru:
Elektrotechnika, elektronika, optoelektronika a fotonika

Jméno uchazeče: RNDr. Radan Slavík, PhD.

Pracoviště uchazeče: ÚFE AV ČR, v.v.i.

Místo a datum: Praha, 17. březen, 2008

## Table of contents

## *Abstract*

*The thesis is dedicated to the field of all-optical signal processing, which should allow for considerably higher processing speed comparing to electronics-based systems. However, compared to electronics, photonics signal processing is at its very beginning.*

*The author with collaborators constructed the first ultrafast all-optical all-fiber temporal differentiator that operates over arbitrary optical waveforms at terahertz speeds. This device may form one of the basic building blocks in the future photonics circuits. Moreover, it can be readily used for various simple pulse shaping and signal processing applications. As an example, we used it to generate a sub-picosecond odd-symmetry Hermite-Gaussian (OS-HG) waveform, which is of particular interest for next-generation optical communications. We also demonstrated theoretically that filter which uses the same technology (long period fiber gratings) can be designed to perform arbitrary-order temporal differentiation. Further, we suggested and demonstrated another configuration for the ultrafast temporal all-optical differentiator that is based on Mach-Zehnder interferometers.*

*We discovered that the implemented all-optical differentiator could be, under certain circumstances, used as a flat-top pulse shaper that reshapes an input pulse generated by a mode-locked laser into a pulse with a square-like (flat-top) temporal waveform. This represents an original filtering scheme never used before in the domain of photonics. We demonstrated that our technique enables an easy generation of very short (picosecond and even sub-picoseconds) flat-top waveforms that have not been generated by any other all-fiber technology so far. Moreover, we found that our scheme can be customized to tolerate certain level of dispersion via tuning of the filter that we developed, which is essential when using sub-picosecond level pulses: such pulses are severely distorted even when propagated through tens of centimeters of a standard optical fiber. We demonstrated that the developed technique is capable of operation in single-channel telecommunications systems operating at 320 and 640 GHz repetition rates.*

*We made a further step that is supposed to substantially broaden the capability of the developed components, which is an incorporation of optical gain. In direct analogy with electrical signal processing, this would enable new schemes to me implemented.*

## 1. Introduction

The implementation of signal processors for all-optical computers and next-generation fiber-optics networks could help overcome the speed limitations that are currently imposed by electronics-based systems [1,2]. All-optical systems offer the potential for larger bandwidth, allowing for processing speeds up to ≈ 40 terahertz – the available bandwidth in an optical fiber in the low-loss telecommunication spectral range from 1300 nm to 1600 nm – compared to a few gigahertz for electronic systems. However, in photonics, there are still no equivalents of fundamental devices that form basic building blocks in electronics, where most of the necessary functionalities such as logic operations, differentiation, and integration can be realized using a simple combination of operational amplifiers, resistors, and capacitors. Thus, the design and realization of the basic building blocks that would perform these logic operations over ultrafast optical waveforms is a necessary step towards the practical realization of multi-functional all-optical signal processors.

Besides the future complex all-optical circuits based on integration of a large number of basic building blocks, there are various applications in which a simple all-optical signal processing functionality is necessary. This is typical for ultrafast optical communications [3], shaping [4] and analysis [5] of ultrashort optical pulses, non-linear optics [6], etc.

The present work on ultrafast all-optical signal processing covers both domains described above. In particular, the author with collaborators constructed the first ultrafast all-optical all-fiber temporal differentiator [A1] that operates over arbitrary optical waveforms at terahertz speeds. Most importantly, this device may form one of the basic building blocks in the future photonics circuits. Beside that, it can be readily used for various simple pulse shaping and signal processing applications. As an example, we applied our differentiator to re-shape an input Gaussian-like optical pulse into a sub-picosecond odd-symmetry Hermite-Gaussian (OS-HG) waveform [A1], which is of particular interest for next-generation optical communications [7,8]. To our knowledge, these experiments represent the first demonstration of direct generation of this complex temporal waveform in the sub-picosecond regime using an all-fiber setup. To accomplish the task of all-fiber all-optical differentiator, we developed an original technique of tuning of long period fiber grating based filters that are used in the studied

configuration [A2]. Unlike previously-reported techniques [9,10], our approach make it possible to attain the resonance condition precisely, which is necessary for proper function of our optical differentiator. Following that, we demonstrated theoretically that filter which uses the same technology (long period fiber gratings) can be designed to perform even arbitrary-order temporal differentiation [A3]. To reach this goal, multiple phase shifts placed at specific positions along the grating have to be introduced. We also suggested and demonstrated other configuration for the ultrafast temporal all-optical differentiator based on Mach-Zehnder interferometers [A4]. This scheme can be extended to obtain higher-order temporal differentiations. In [A4], this was demonstrated for the second-order temporal differentiation, which was the first demonstration of terahertz-bandwidth higher-order differentiation in the literature.

We found that the implemented all-optical differentiator could be, under certain circumstances, used as a flat-top pulse shaper that reshapes an input pulse generated by a mode-locked laser into a pulse with a square-like (flat-top) temporal waveform [A5]. This represented an original filtering scheme never used before in the domain of photonics. The existing schemes were predominantly based on sinc-like pulse spectrum shaping (sinc(x)=sin(x)/x) [11] or on the effect of all-optical frequency-to-time mapping [12]. Although only some of these techniques have principal limitations in scaling to faster waveforms, none of them was demonstrated in any system operating at repetition rates over 160 GHz (requiring flat-top waveforms of several picosecond long). On the contrary, our technique enables an easy generation of very short (picosecond and even sub-picoseconds) flat-top waveforms that have not been generated by any other all-fiber technology so far, as it is based on the developed differentiator that operated over a very large bandwidth. Moreover, we found that the developed technique can be customized to tolerate certain level of dispersion [A6] via tuning of the filter that we developed [A7], which is essential when using sub-picosecond level pulses: such pulses are severely distorted even when propagated through tens of centimeters of a standard optical fiber. All these features were necessary to construct advanced ultrafast all-optical components for the next-generation ultrahigh capacity optical communications [A8, A9]. We demonstrated that our technique is capable of operation in single-channel telecommunications systems operating at 320 and 640 GHz repetition rates [A8,A9]. We reiterate that the other reported techniques were demonstrated at repetition rates up to 160 GHz only [11,12]. As our devices appeared to be capable of

operating even at repetition rates of 640 GHz, they are planned to be implemented in various ultrahigh capacity systems in COM Research Center, Technical University of Denmark and Fraunhofer Heinrich Hertz Institute in Berlin, which are two out of three laboratories in Europe that demonstrated telecommunication systems operating at 640 Gbit/s per channel and above so far.

All this above-mentioned work is supposed to be substantially broadened by using all-optical filters that incorporate gain [A10]. The optical gain can be used for tuning of the developed devices and/or can allow new filter capability to me implemented – in direct comparison with electrical filters. Besides that, there is an obvious advantage of mitigating signal loss. This topic is – concerning all-optical signal processing - at a very beginning, as optical fibers and waveguides with high enough gain have started to appear only very recently.

## 2. All-optical differentiation

Several schemes for performing real-time derivation in the optical domain have been previously proposed at the theoretical level [13,14]. The experimental device demonstrated by us has been realized according to a novel all-fiber design recently proposed [14], which is based on the use of a single *uniform* long-period fiber grating and is suitable for operation over the entire bandwidth of arbitrary signals with sub-picosecond temporal features (corresponding bandwidths of a few terahertz). The main advantages of the realized device are inherent to all-fiber-based devices, namely simplicity, relatively low cost, low loss, and full compatibility with fiber optics systems.

The underlying concept of the studied component is based on the fact that the spectrum associated with the derivative of the temporal envelope of a given signal centered at frequency $\omega_{car}$ (carrier frequency) $E(\omega-\omega_{car})$ (represented in the Fourier domain) is given by $i(\omega-\omega_{car})E(\omega-\omega_{car})$ [15], Fig. 1, where $\omega$ is the optical frequency, and $\omega-\omega_{car}$ is the base-band frequency. Thus, a first-order temporal differentiator is essentially a linear filtering device that provides the following spectral transfer function, Fig 1:

$$H(\omega-\omega_{car}) = i(\omega-\omega_{car}) \qquad (1)$$

Consequently, the two key features of the filter's transmission are (i) it depends linearly on the base-band frequency, and (ii) it is zero at the signal central frequency $\omega_{car}$. It is worth noting that these two key features imply an exact $\pi$ phase shift across the filter central frequency $\omega_0$ aligned to yeld $(\omega_0-\omega_{car})$. The ideal complex transmission of an optical differentiator is schematically shown in Fig. 2 (dash-dot green line).

The required energy depletion at the signal central frequency can be produced by resonance-induced complete energy transfer elsewhere. Specifically, in waveguide optics, this can be achieved by resonant transfer of light between two spatially close waveguides, or between two modes of the same waveguide (e.g. cladding and core modes of an optical fiber). Resonant light coupling is induced when the light propagates through both waveguides (modes) with identical speeds, which is practically attainable e.g. by an increase or decrease of the light speed in one of the waveguides (modes) using a suitable diffraction grating [16]. The specific diffraction grating used in our experiments, which is realized as a periodic change of the refractive index along the direction of light propagation within a single waveguide (optical fiber), induces resonant coupling between two co-propagating modes and is commonly called *long-period fiber grating* (LPG) [17]. The term 'long' refers to its period, which typically varies from tens to hundreds of micrometers, in contrast to short-period gratings (Bragg gratings), where the light is backscattered, resulting in coupling between modes traveling in opposite directions (in a Bragg geometry, the corrugation period is approximately half the optical wavelength, micrometers or less [16]).

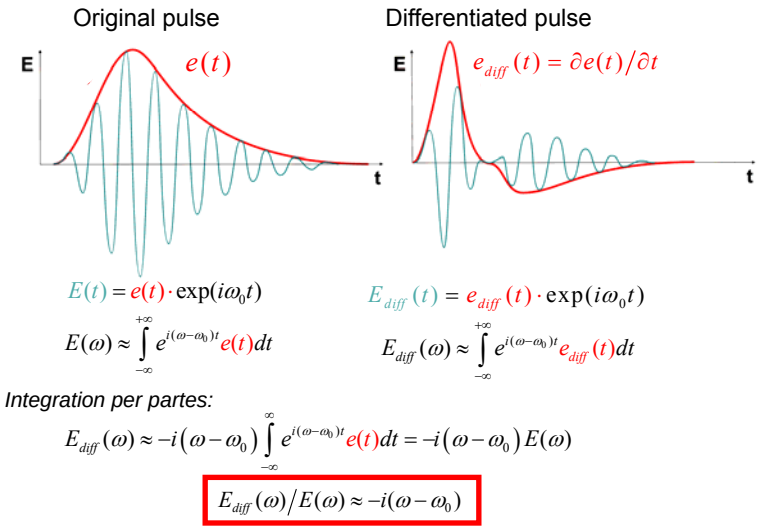


Fig. 1. Principle of the optical differentiator.

An optical fiber-based LPG induces gradual coupling at a rate of $\kappa$ per unit length between the core guided mode and cladding mode(s) [17]. To obtain efficient coupling between these modes, the period of the LPG must be properly adjusted to cause light diffraction from the core mode into the chosen cladding mode. Due to the different dispersion slopes of these two modes, the resonant coupling occurs only at a specific frequency $\omega_0$, referred to as the LPG resonance frequency. It is known that if the device is designed to exactly satisfy the condition $\kappa L = \pi/2$ ($L$ is the grating length, $\kappa$ is the coupling coefficient, and $\kappa L$ is the LPG strength), the grating induces a total (100%) energy coupling from the input guided core mode into the cladding mode (at $\omega_0$) [17]. It was shown recently that an optical fiber-based LPG specifically designed to provide 100% coupling between the fiber core mode and one of its cladding modes at the resonance frequency provides both the required $\pi$ phase shift and the linear dependence of transmission that is necessary for first-order time differentiation (assuming that the input optical signals are centered at the LPG resonance frequency) [14]. Such an LPG, coincidentally, has the required spectral linear response over a bandwidth as broad as several terahertz.

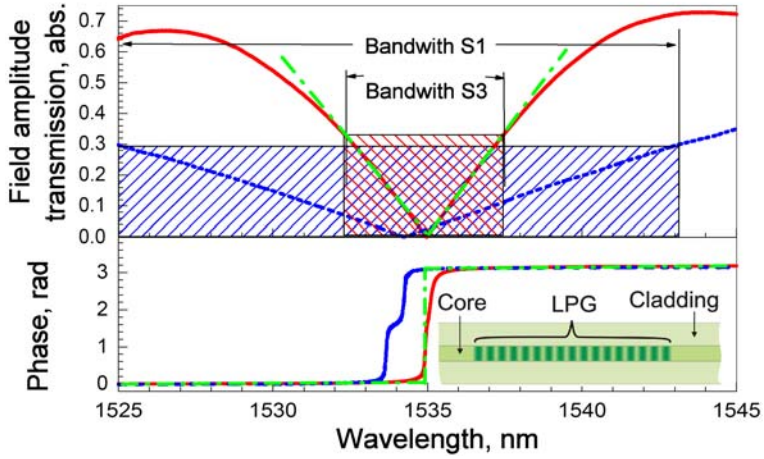


Fig. 2. Amplitude and phase characteristics of the fiber LPG filters. Measured field amplitude and phase characteristics of the realized long, S3 (red) and short S1 (blue) LPGs together with the theoretical characteristics of an ideal differentiator similar to S3 (green, dash-dotted lines). The S3 and S1 LPG operational bandwidths (highlighted in the figure) are 5.5 nm and 19 nm, respectively. The inset shows a fiber uniform LPG, where the level of green corresponds to the refractive index.

The transfer function of the realized LPG samples is shown in Fig. 2 [A1, A2]. We see that it can perform optical differentiation within a certain bandwidth around the resonance frequency. Subsequently, we performed a proof-of-principle experiment, in which we differentiated 700-fs FWHM Gaussian-like pulses – the result is shown in Fig. 3 [A1]. For comparison, the expected shape of the complex differentiated waveform is also shown. We conclude that the developed devices perform the desired temporal differentition functionality with high accuracy.

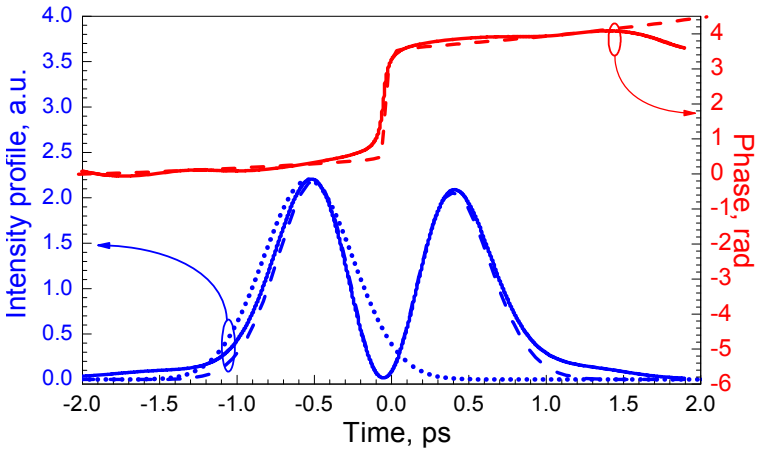


Fig. 3. Results from Spectral Interferometry (SI) measurements. The phase (red) and intensity (blue) temporal profiles of the generated odd-symmetry HG waveform are retrieved from the experimental data obtained using Fourier-Transform SI (solid lines); the theoretical prediction (dashed lines) and considered input pulse waveform (dotted line) are also shown.

We demonstrated that the used scheme may be extendable for higher-order differentiation, using similar approach as that recently-reported for reflection-operating fiber Bragg gratings [18]. The $N$-th order temporal differentiation is mathematically described as $\partial^n u(t)/\partial t^n$, where $u(t)$ is complex envelope of an input signal. The corresponding spectrum can be expressed as $(-i(\omega-\omega_0))^N U(\omega)$, where $U(\omega)$ is spectrum of $u(t)$. Thus, optical differentiation of the $N$-th order can be obtained by a filter that has the transfer function of $(-i(\omega-\omega_0))^N$. Considering expansion of the filter transfer function into Taylor series around $\omega_0$:

$$f(\omega-\omega_0)=f(\omega_0)+\left(f(\omega-\omega_0)\right)'(\omega-\omega_0)+0.5\left(f(\omega-\omega_0)\right)''(\omega-\omega_0)^2+\ldots \qquad (2)$$

we are looking for a filter with transfer function that has only the $(n+1)$-th Taylor series term with other terms being much smaller (ideally zero).

Here, we consider LPG consisting of multiple segments, each of them formed by a uniform LPG. For example, when considering two segments, there are two LPG strengths as parameters and one can try to look for a transfer function that has the constant and linear Taylor series terms equal to zero. Provided the higher-order Taylor series terms are much smaller than the quadratic one, such filter should perform the second-order differentiation. The two gratings can be connected via a $\pi$

phase shift, which leads (as will be shown later) to mathematically the least complicated form. This approach can be further applied for obtaining *N*-th order differentiation by using *N*–1 $\pi$ phase shifts [A3].

As follows from [14], a uniform LPG (corresponding to the *j*-th segment of our LPG) is described by the transfer matrix:

$$\mathbf{F}_j = \begin{bmatrix} \cos(\gamma L_j) + i\frac{\sigma}{\gamma}\sin(\gamma L_j) & i\frac{\kappa}{\gamma}\sin(\gamma L_j) \\ i\frac{\kappa}{\gamma}\sin(\gamma L_j) & \cos(\gamma L_j) - i\frac{\sigma}{\gamma}\sin(\gamma L_j) \end{bmatrix}. \qquad (3)$$

Here, $\gamma = \sqrt{\kappa^2 + \sigma^2}$, $\kappa$ is the coupling coefficient between the core mode and a chosen cladding mode (determined by the period $\Lambda$ of the LPG for a given wavelength), σ is the detuning factor given by $\sigma = (\beta_1 - \beta_2)/2 - \pi/\Lambda$ ($\beta_1$, $\beta_2$ are the propagation constants of the core mode and the cladding mode, respectively) and $L_j$ is the length of the j-th LPG segment. The π phase shifts between consecutive LPG segments were introduced via the matrix:

$$\Phi = \begin{bmatrix} e^{(-i\pi/2)} & 0 \\ 0 & e^{(+i\pi/2)} \end{bmatrix} = \begin{bmatrix} i & 0 \\ 0 & -i \end{bmatrix} \qquad (4)$$

and the overall transfer characteristics of the system was computed as

$$\mathbf{F} = \mathbf{F}_n \cdot \Phi \cdot \mathbf{F}_{n-1} \cdot \Phi \cdots \Phi \cdot \mathbf{F}_2 \cdot \Phi \cdot \mathbf{F}_1 . \qquad (5)$$

As we see from (3), using $\pi$-phase shifts leads to the matrix $\Phi$ that does not have complex elements (elements with both real and imaginary parts), which simplifies significantly the mathematical description.. Considering that the input and output signals are propagating in the fiber core mode, the filter field transfer function is characterized by **F**(1,1) element. We expanded the **F**(1,1) into Taylor series analytically around the center frequency $\omega_0$. Then, for an $N^{th}$ order differentiator we require the first *N* terms to be equal to zero. It creates the set of *N* equations to be solved to find *N* LPG segment lengths. The results [A3] in terms of complex field transfer function are shown in Fig. 4 together with the transfer function of an ideal *N*-th order differentiator for *N* =2, 3, 4, and 5 (the linear term of the phase response that corresponds to a simple non-dispersive propagation is adjusted to enable comparison between

the ideal and LPG-based differentiators); the temporal response is shown then in Fig. 5. For Figs. 4 and 5, we considered experimentally obtainable coupling coefficient $\kappa$=120 $m^{-1}$, SMF-28 fiber and coupling to the 7$^{th}$ cladding mode (4$^{th}$ odd cladding mode) at the frequency of 193.5 THz (1550 nm), which requires LPG period of 495 μm.

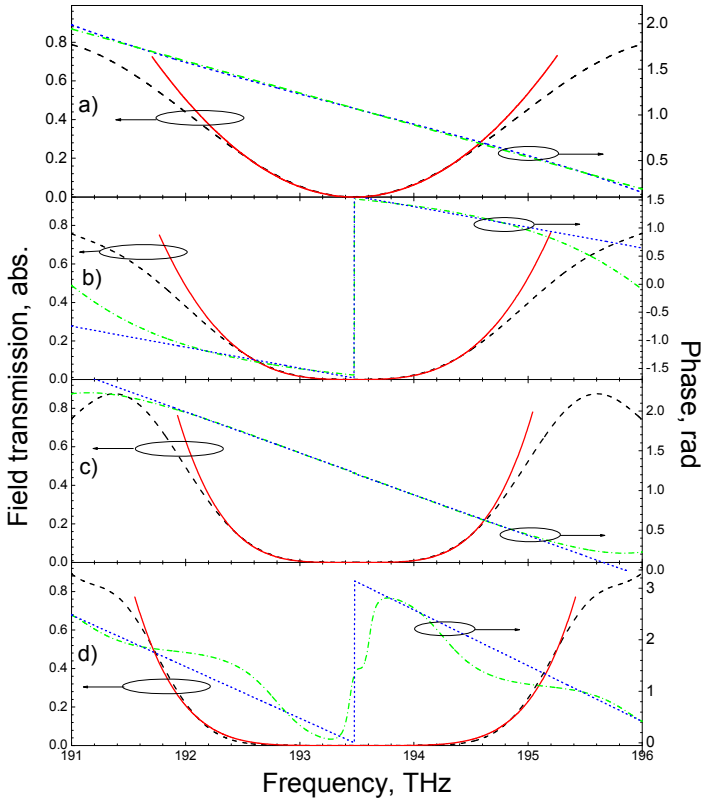


Fig. 4 Transfer functions of the designed $N$-th order temporal differentiators with $N$ = 2 (a), 3 (b), 4 (c), and 5 (d) (black, dot) and corresponding ideal differentiator characteristics (with $(\omega_{opt}-\omega_0)^N$ dependence) (red, solid). Phase dependencies are shown as green, solid lines (designed differentiators) and as blue, dot lines (ideal differentiators with linear term (that corresponds to a non-dispersive propagation time delay) adjusted to enable direct comparison with the designed differentiators).

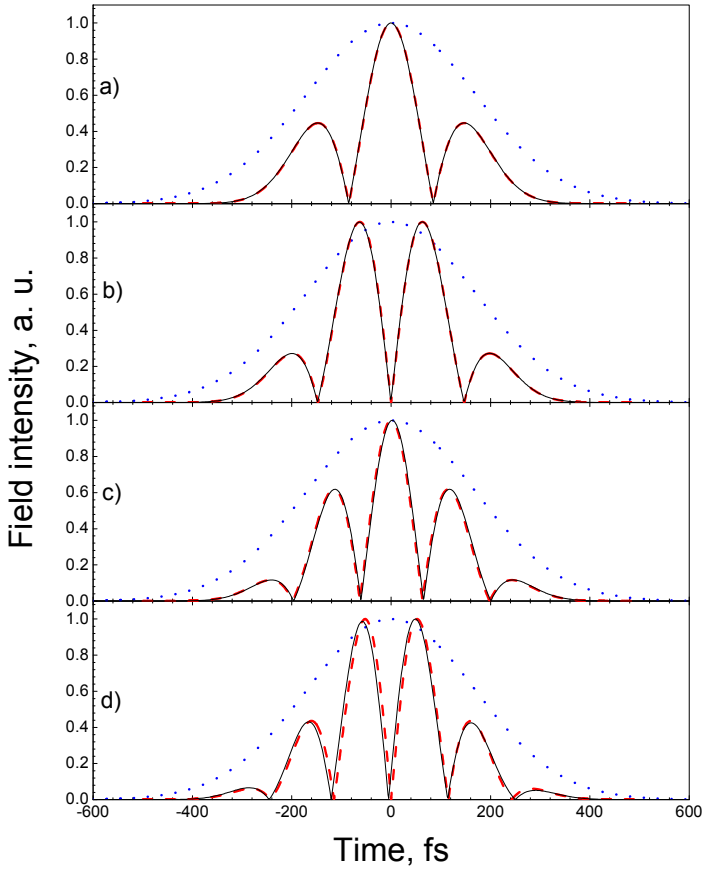


Fig. 5 The temporal envelopes of an input Gaussian pulse (dotted, blue) and of the waveform at the LPG output (for the 2nd (a), 3rd (b), 4th (c) and 5th (d) order differentiator) (solid, black) and ideal waveforms of differentiated pulses (dashed, red).

We suggested also an alternative technique for the all-optical ultrafast differentiation that is based on a two arm interferometer [A4] that can be implemented using of-the-shelf bulk optics based components [A4] or using wavegude technology.

The device is demonstrated on a symmetric Michelson interferometer, which has the spectral transfer function given by:

$$H_t(\omega-\omega_0)\approx 1+\exp(i\omega\tau)=1+\exp\left[i(\omega-\omega_0)\tau\right]\exp(i\omega_0\tau), \qquad (6)$$

where $\tau$ is the relative time delay between the two interferometer arms. Setting the interferometer to operate at a minimum transmission $t(\omega-\omega_0) = 0$ at the carrier frequency ($\omega = \omega_0$), it follows from (6) that $\tau = \pi(2m+1)/\omega_0$ ( $m$ is an arbitrary integer) and subsequently:

$$H_t(\omega-\omega_0) \approx 1-\exp\left[i\pi(2m+1)(\omega-\omega_0)/\omega_0\right], \qquad (7)$$

The function in (7) can be approximated over a sufficiently narrow bandwidth centered at $\omega_0$ by the first two terms of the Taylor series resulting in:

$$H_t(\omega-\omega_0) \approx -i(\omega-\omega_0)\pi(2m+1)/\omega_0, \qquad (8)$$

which is the transmission function required for the 1st order temporal differentiation.

The simulated spectral magnitude and phase response of a single Michelson interferometer over a half of its period is shown in Fig. 6 (solid curves). We fixed the relative time delay to $\tau$ = 600 fs corresponding to $m$ = 116. It can be observed that as anticipated, the interferometer frequency response is linear only within the vicinity of the zero transmission wavelength. As the $N^{th}$-order differentiator can be made using a linear filter with the transfer function of $[i(\omega-\omega_0)]^N$, it can be realized by a concatenation of $N$ identically-configured single-stage interferometers. The dashed curves in Fig. 6 show the result for $N = 2$ (the 2nd-order optical differentiator), which is characterized by a quadratic frequency amplitude response; notice that the operation bandwidth is identical to that of the corresponding 1st order differentiator. The differentiation capabilities of the constructed first and second-order differentiators [A4] are shown in Figs. 7 and 8.

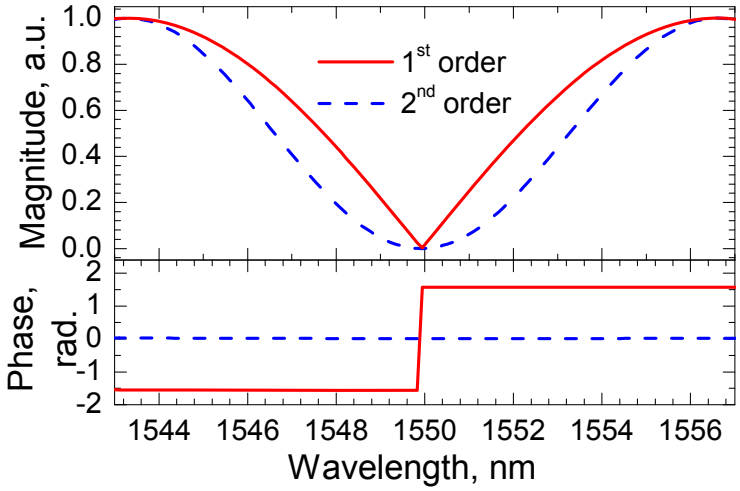


Fig. 6. Simulated magnitude and phase of the spectral transmission $t$ for a single and double Michelson interferometer (parameters given in the text) over a half of its period.

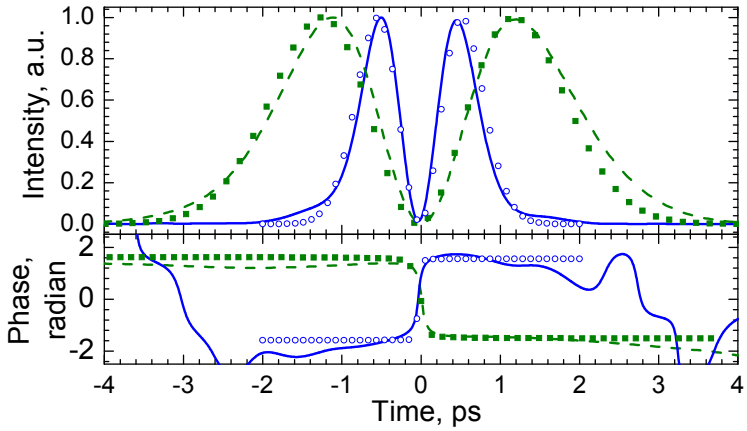


Fig. 7. Measured 1st order differentiated pulses generated from 1.9 ps (dashed curves) and 0.9 ps (solid curves) Gaussian-like pulses; ticks show the exact differentiation characteristics of an ideal Gaussian pulses.

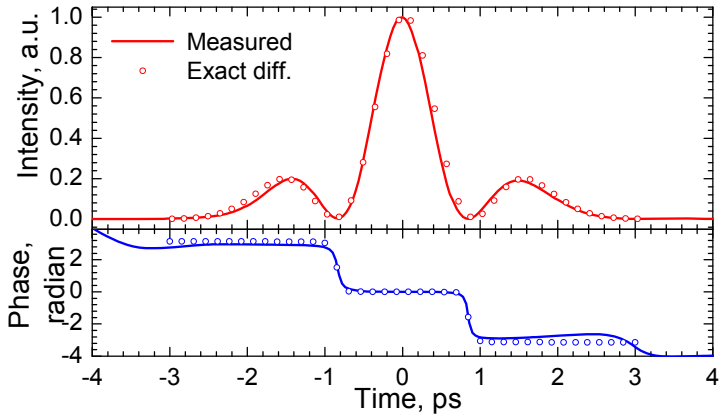


Fig. 8. Measured 2nd order differentiated pulse using a 1.2-ps input Gaussian-like pulse; hollow circles show exact differentiation characteristics of an ideal Gaussian pulse.

## 3. Ultrashort flat-top pulse generation

As we have shown in the previous chapter, a uniform LPG operating in full-coupling condition (e.g. when $\kappa L = \pi/2$ [14] provides a linear filtering function around its resonance frequency $\omega_0$). In what follows, we assume an input Gaussian pulse, $u(t) \propto exp(-at^2)$, where $a$ is a constant of no relevance for our purposes. The corresponding differentiated pulse is an odd-symmetry Hermite-Gaussian (HG) waveform [14,19], $\partial u(t)/\partial t \propto t \cdot \exp(-at^2)$, which consists of two concatenated pulses with identical amplitude profiles inversed in time that have a relative phase difference of $\pi$. Let us now consider a finite detuning of the input pulse carrier frequency $\omega_{car}$ with respect to the filter's resonance frequency $\omega_0$, $\Delta\omega=\omega_{car}-\omega_0$. The LPG filtering function is now given by $V(\omega) \propto -i\omega U(\omega) + i\Delta\omega\, U(\omega)$, which in the temporal domain corresponds with the following operation: $v(t) \propto \partial u(t)/\partial t + i\Delta\omega\, u(t)$. Thus, the temporal intensity profile of the signal at the LPG output can be written as:

$$|v(t)|^2 \propto |\partial u(t)/\partial t|^2 + \Delta\omega^2 |u(t)|^2 . \qquad (9)$$

From (9) it is obvious that for $\omega_{car} = \omega_0$ the device operates as an optical differentiator. However, for $\omega_{car} \neq \omega_0$, $|v(t)|^2$ consists of the sum of the differentiated waveform and the original waveform, with a relative weight given by the detuning factor $(\omega_{car} - \omega_0)^2$. When $|u(t)|^2$ is a temporally symmetric pulse (like a $Sech^2$ or a Gaussian), the differentiated pulse is a symmetric double-pulse [A1]. By properly adjusting the detuning factor $(\omega_{car} - \omega_0)^2$, the valley in between the two peaks of the double-pulse (differentiated waveform) can be completely filled with the contribution coming from the second term of the right side of (9) (which has the shape of the original pulse *u(t)*) leading to the formation of a single flat-top pulse, Fig. 9 [A5].

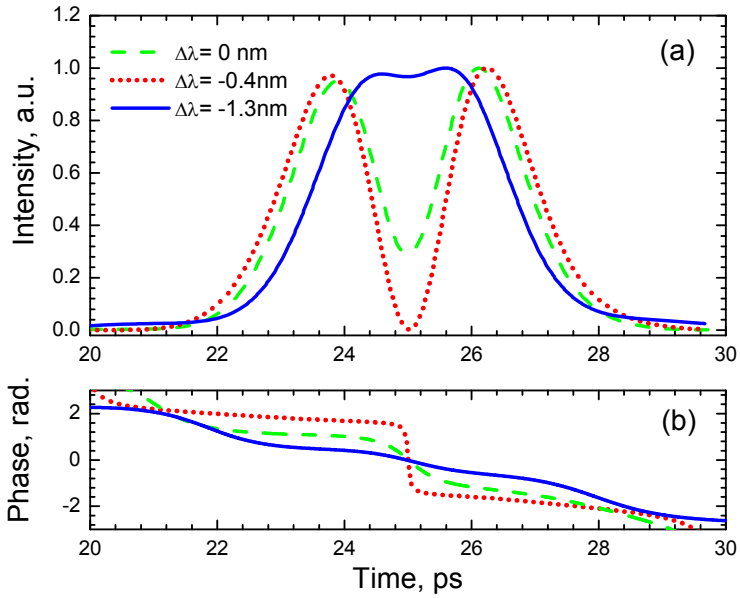


Fig. 9. Experimentally generated intensity (a) and phase (b) temporal profiles of the synthesized waveforms at the uniform LPG output for different values of the 1.8-ps input pulse-LPG detuning $\Delta\lambda$.

In the presence of the first-order chromatic dispersion *D*, the original, transform-limited waveform *u(t)* changes to:

$$u(t)^{disp} \propto w(t)\exp(-jDt^2), \tag{10}$$

where *w(t)* is a real (transform-limited) function. For example, for *u(t)* Gaussian, *w(t)* is also of Gaussian shape of longer duration. As a result, (9) can be re-written as:

$$\left|v(t)^{disp}\right|^2 \propto \left|\partial w(t)/\partial t\right|^2 + \left|w(t)\right|^2\left(\left(\omega_{car}-\omega_0\right)-2Dt\right)^2 \tag{11}$$

By comparing (11) with (9) we see that besides *u(t)* being replaced by *w(t)*, the so-called detuning factor has been modified to $((\omega_{car}-\omega_0)-2Dt)^2$, which depends on the time variable due to the presence of the introduced term *Dt*. This term is odd-symmetric in *t* (i.e. it is negative for *t<0* and positive for *t>0* with the same absolute value for $\pm|t|$), thus inducing an asymmetric distortion in the otherwise temporally symmetric output pulse waveform. It is worth noting that the term *Dt* does not cause the mentioned asymmetric distortion in (11) when the device is operated as an optical differentiator, which corresponds to $\left(\omega_{car}-\omega_0\right)=0$.

We suggested to compensate for this dispersion-induced distortion by proper tuning of the LPG. In what follows we provide a brief analysis that predicts that the dispersion-induced distortion of a flat-top pulse generated with an LPG-based optical differentiator could be compensated by properly adjusting the LPG strength $\kappa L$..

According to a previous study [14], the transfer function of a LPG that is set to operate close to the full coupling condition (zero transmission at the resonance frequency $\omega_0$) can be approximated in the vicinity of the resonance frequency as:

$$H(\omega) \approx \left[\cos(\kappa L) + j\alpha(\omega-\omega_0)\sin(\kappa L)\right]\exp(j\beta L), \tag{12}$$

where $\alpha$ is a constant, and $\beta$ is the core mode propagation constant. Now, let us consider a slight detuning $\Delta\kappa$ in the LPG coupling coefficient with respect to the value for which the LPG operates as optical differentiator ($\kappa L = \pi/2$). Considering the first two terms of the corresponding Taylor series, we rewrite (12) into:

$$H(\omega) \approx \left[\Delta\kappa L + j\alpha(\omega-\omega_0)\right]\exp(j\beta L) \tag{13}$$

For the sake of simplicity, we will first consider zero detuning between the input pulse carrier frequency $\omega_{car}$ and the filter central frequency $\omega_0$; in this case, the filtering operation in the temporal domain is given by:

$$v(t) \approx \alpha \frac{\partial u(t)}{\partial t} + \Delta\kappa L u(t) \,. \tag{14}$$

The key aspect of (14) is that there is no phase difference between the two terms on the right hand side, so the output intensity includes an interference term. For a transform-limited input optical pulse (with real temporal envelope) we obtain:

$$\left|v(t)\right|^2 \approx \alpha^2 \left|\frac{\partial u(t)}{\partial t}\right|^2 + \left|\Delta\kappa L u(t)\right|^2 + 2\alpha\Delta\kappa L \frac{\partial u(t)}{\partial t} u(t) \,. \tag{15}$$

Further assuming that the input pulse is temporally symmetric (e.g. Gaussian or Sech$^2$), the last term in (15) exhibits temporal odd symmetry (i.e. it is negative for $t<0$ and positive for $t>0$ with the same absolute value for $\pm|t|$), thus inducing a temporally asymmetric waveform distortion similar to that caused by the dispersion (see discussions above). This odd symmetry comes from the differentiated waveform ($\partial u(t)/\partial t$) that consists of two pulses that have identical temporal field profiles (inverted in time), but are phase shifted by $\pi$. This $\pi$-phase shift implies that the field intensities of the two pulses are of opposite signs [A1]. As a result, (15) indicates that depending on the sign of $\Delta\kappa$, the leading-edge peak of the generated optical pulse will exhibit a higher intensity ($\Delta\kappa>0$) or a lower intensity ($\Delta\kappa<0$) than that of the trailing-edge peak.

When considering (i) a finite detuning of the pulse carrier frequency $\omega_{car}$ from the filter central frequency $\omega_0$ and (ii) the effect of dispersive propagation, we obtain an equation that includes two asymmetry terms – one that is associated with the pulse dispersive propagation (present in (11)) and another one that is associated with the effect of LPG strength tuning (present in (15)):

$$\left|v(t)^{disp}\right|^2 \propto \alpha^2 \left|\frac{\partial w(t)}{\partial t}\right|^2 + \Delta\kappa^2 L^2 \left|w(t)\right|^2 + 2\alpha\Delta\kappa L w(t) \frac{\partial w(t)}{\partial t} + \tag{16}$$

$$+\alpha^2\left((\omega_{car}-\omega_0)-2Dt\right)^2\left|w(t)\right|^2.$$

By a proper choice of the sign and magnitude of $\Delta\kappa$, the two asymmetry terms in (16) can, to a certain degree, cancel each other out. In this way, the dispersion-induced waveform asymmetry could be compensated by a proper tuning of the LPG strength (to operate outside the full-coupling condition). As follows form results shown in Fig. 10 [A6], our numerical simulations and experimental results show that the dispersion-induced waveform distortion can be counter-balanced almost entirely using this simple mechanism even in the presence of a significant amount of the dispersion.

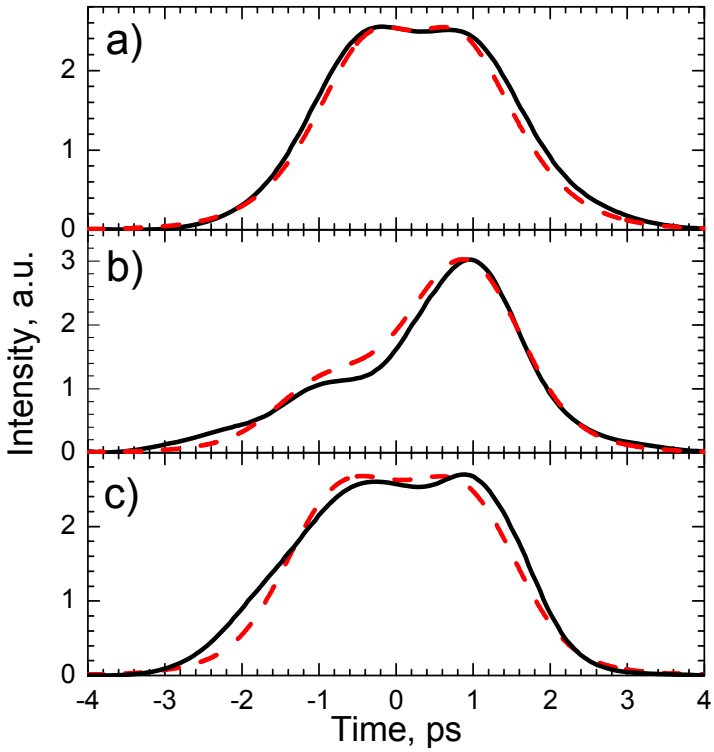


Fig. 10 Waveforms at the output of the LPG filter adjusted to obtain flat-top waveform (a); situation shown in (a) after adding 18 meters of SMF-28 standard telecom fiber (b); and situation from (b) after re-adjusting the LPG strength and filter-input pulse detuning to recover the flat-top waveform (c). Calculated data shown as dashed red; measured as solid black.

## 4. Ultrafast telecommunications

For high-speed serial data transmission that operates at rates of 160 Gbit/s and above, management of the timing jitter becomes increasingly challenging. The tremendous impact of timing jitter can be reduced by use of system components (e.g., switches, demultiplexers, add-drop, etc.) with a high tolerance to the timing jitter. High-speed, jitter-tolerant optical components may be obtained, e.g. by generating a square-like, i.e. flat-top gating window in ultra-fast (fs-response) Kerr-effect-based non-linear optical components. This scheme was implemented, e.g., using a non-linear optical loop mirror (NOLM) [20]. For optimum performance, the gating pulse has to be shorter than the one-bit time window and at the same time it should have constant intensity over a time interval as long as possible. Both of these requirements can be fulfilled when using flat-top pulses.

Fig. 11 shows a schematic of the experimental set-up. It consists of three principal parts that will be described subsequently: the NOLM, the flat-top pulse generator, and the transmitter.

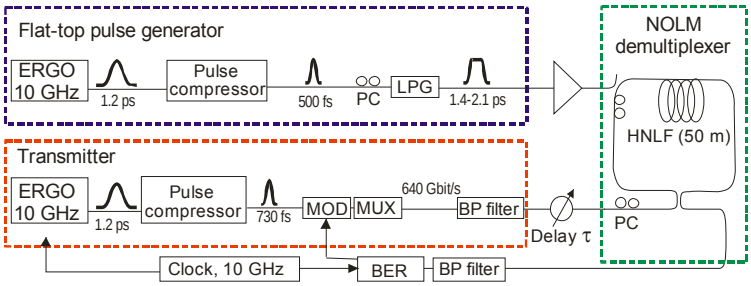


Fig. 11. Set-up for 640 Gbit/s. ERGO – Erbium glass oscillator, PC – polarization controller, MOD – modulator, BER – bit error ratio, BP – band pass.

The NOLM consists of a *Sagnac* interferometer containing a non-linear fiber. The signal propagates inside the loop in both (opposite) directions and interferes at the NOLM's input/output coupler. Without the presence of the gating signal, the phase difference experienced by light propagating in both directions is zero, which results in constructive interference at the input port of the NOLM, i.e. the signal is reflected back. In the presence of the gating pulse that propagates unidirectionally in the NOLM only, the co-propagating signal light experiences a non-linear phase shift, which introduces a phase difference between signals

propagating in both directions. Adjusting the parameters (e.g., the gating signal intensity) to produce a phase difference equal to $\pi$, the signal, which is overlapped with the gating pulse, is directed to the NOLM output port. For optimum operation, the gating signal has to be propagated simultaneously with the target data pulse. Obviously, any delay between these two pulses (caused, e.g., by the timing jitter) severely degrades the performance. As the tolerance to the timing jitter scales with the one-bit time slot duration, higher repetition rate based systems are generally more timing jitter sensitive.

For the system evaluation, we measure the back-to-back sensitivity at 10 Gbit/s first. Subsequently, we characterize the 640-Gbit/s set-up: we measure power penalty using the optical gate based on the flat-top pulses and for comparison with a non-flat-top pulse, Fig. 12. The flat-top pulses are generated usign previously-described pulse shaping scheme [A5,A6]. To performe fine tuning of the filter resonance frequency and the LPG strength independently, we developed an original tuning technuque based on simultaneous bending and straining of a fiber with inscribed LPG [A7]. From Fig. 12 we see that the use of non-flat-top gating pulses results in an additional power penalty of 13 dB for the error-free level of BER=$10^{-9}$ compared to the flat-top case, where the penalty is only 3.5 dB with respect to the 10 Gb/s back-to-back. Moreover, there is an error floor using non-flat-top pulses indicating that the system is limited by relative timing jitter, which is over 110 fs rms in our system This is confirmed by the eye diagrams that are shown in Fig. 13. We clearly see that using the non-flat-top gating pulses lead to amplitude noise, which is typical for timing jitter-limited systems. Again, influence of this phenomenon is considerably reduced when flat-top gating pulses are used. All these measurements were carried out on the same data channel.

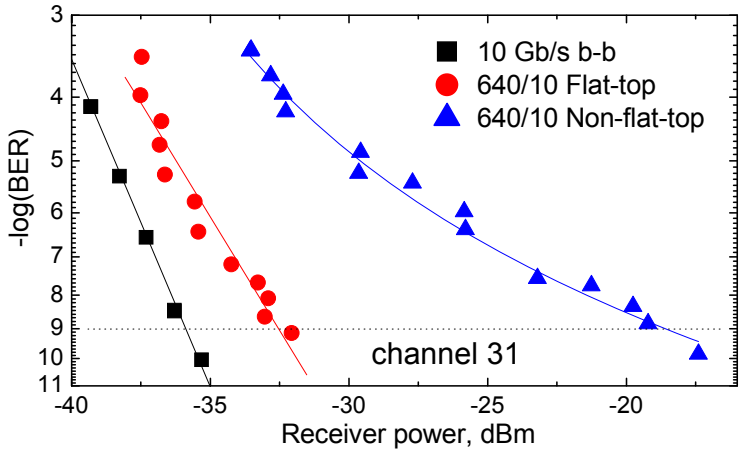


Fig. 12. BER characteristics: back-to-back (squares), using flat-top pulses (circles), and using non-flat-top pulses (triangles). The demultiplexing results are from the same data channel.

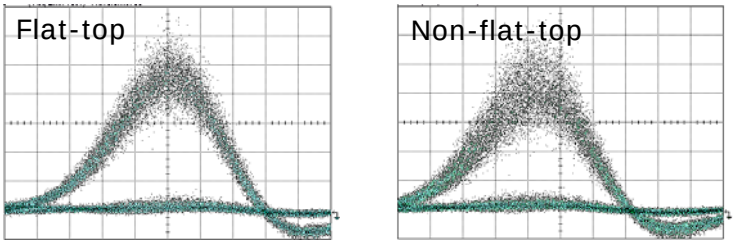


Fig. 13. Eye diagrams obtained for flat-top and non-flat-top gating pulses.

The previous data clearly show that the used flat-top gating pulses are capable of mitigating the system timing jitter being over 110 fs rms. To find a maximum value of the timing jitter that can be tolerated by the demultiplexer with the available flat-top pulses, we increase the power at the receiver by 5 dB over the error-free level and vary the delay between the data and gating pulses. Subsequently, we measure the BER for different levels of this delay, Fig. 14. The flat-top waveform is also shown in order to visualize the relation between the gating pulse flat-top duration and the amount of delay that can be tolerated for error-free operation (with BER<$10^{-9}$). We see that an additional time displacement of 350 fs can be tolerated. Together with the system jitter of 110 fs, this gives almost 500 fs tolerance or 30% of the 640 Gb/s time slot, which is

a value very close to the flat part of the flat-top pulse of 550 fs. For non-flat-top gating pulses, the system do not tolerate any additional timing jitter, which can be understood from the above analysis indicating that the system is already limited by its timing jitter of 110 fs rms.

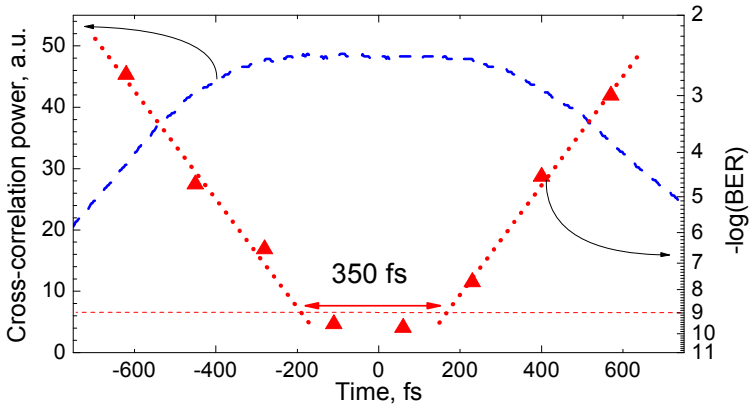


Fig. 14. BER timing jitter tolerance (triangles) and intensity profile of the used flat-top pulse (dashed).

## 5. Gain-assisted components

As we showed in previous chapters, optical filters are needed and routinely used in ultrafast all-optical signal processing. They are based on different principles and technologies like thin film filters, fiber Bragg gratings, arrayed waveguide gratings, cascaded waveguide resonators and interferometers, LPGs, etc. In the current and next-generation optical systems, the tunability of these devices is more and more an imperative to enable systems reconfiguration and fine tuning. Moreover, for further integration, it may be also advantageous to combine filtering functions with signal amplification.

One of possible implementations that could address these issues is based on LPG made into an active optic medium, the idea that was already presented in several reports [21,22,23,24]. Work presented in Refs. 21 and 22, shows how the LPG transmission characteristics would change via optical pumping of erbium ions present in the fiber cladding [21] or core [22] (it is worth noting that similar effects cannot be generally obtained considering a passive LPG followed by an amplifier). It was predicted [21] that total energy transfer from the core into the

cladding mode can be realized not only at the discrete values of the LPG strength $\kappa L=m\pi/2$ ($m$=1,2,3, …) as for an LPG made in a standard low-loss and no gain fiber, but practically for any value of the LPG strength. This may result in a possibility to realize an LPG that has its resonance dip controllable via optical pumping. Concerning realization of LPGs in active optical fibers, the existing reports [23,24] do not demonstrate experimentally any of the above-mentioned effects.

We realized experimentally, to our knowledge for the first time, an LPG-based device that shows advanced features accessible only by incorporation of an LPG into an active media, more specifically (i) tuning of the LPG resonance dip depth and (ii) an amplifying LPG operating in the full coupling condition. Incidentally, this is also the first report on LPG fabrication in an active fiber using $CO_2$ laser technique.

First, let us explain the principal mechanism. The complex amplitude of the core mode, where the signal is initially launched, is in presence of the LPG and optical gain described by the equation [10]:

$$H_t = \left[\cos(\gamma L) + i\frac{\sigma}{\gamma}\sin(\gamma L)\right]\exp\left(i(\beta_{10}-\sigma)L\right), \qquad (17)$$

where $\sigma = (\beta_{10} - \beta_{20} - 2\pi/\Lambda)/2$ is the detuning factor, $\beta_{10} = \beta_1 + i\alpha_1$ is the propagation constant of the core mode, $\beta_{20} = \beta_2 + i\alpha_2$ is the propagation constant of the interacting cladding mode with $\alpha_{1,2}$ accounting for loss ($\alpha_1$ , $\alpha_2$ >0) or gain ($\alpha_1$ , $\alpha_2$ < 0) of the modes.

At the resonance wavelength, at which the mode matching condition is satisfied, the detuning factor becomes purely imaginary: $\sigma = -j(\alpha_2 - \alpha_2)/2$. If we look at the condition at which the transmission is zero at the resonance wavelength, we get from (17) the following condition (for q>-1; for q<-1, the formula changes to a hyperbolic function [21]):

$$\cos\left[\sqrt{1-q^2}\,\kappa L\right] + \frac{q}{\sqrt{1-q^2}}\sin\left[\sqrt{1-q^2}\,\kappa L\right] = 0, \qquad (18)$$

This expression is already re-written to show explicit relation between the LPG strength $\kappa L$ and a dimensionless gain factor $q = (\alpha_2 - \alpha_1)/2\kappa$. Solution of (18) is shown in Fig. 15 - we see that full coupling is possible for almost any value of $\kappa L$ provided the loss/gain of the core and cladding modes are properly adjusted (parameter $q$).

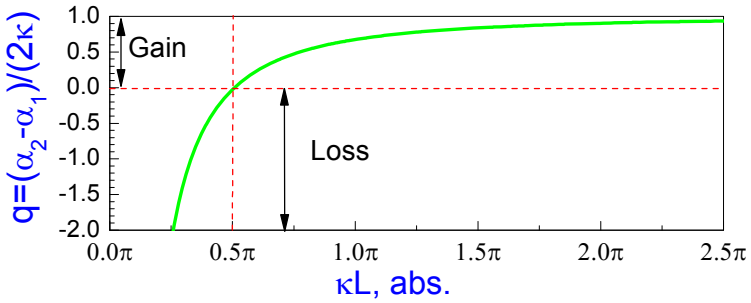


Fig. 15. Optimum values of gain/loss factor $q$ that provide 100% core mode attenuation at the resonance wavelength.

The fact that amplifying fibers (with core doped with $Er^{3+}$ and gain in the 1.55 μm spectral window, EDF) are routinely used in fiber optic telecommunications together with the fact that there are up-to-date no demonstration of this very promising tuning technique are, in our opinion, caused by experimental challenges associated with it.

First, the most usual active fibers are designed for fiber amplifiers and are used in lengths of meters to tens of meters, which would be rather unpractical for a filtering device. Fibers with considerably higher gain are available, but are rarely UV photosensitive, which makes it impossible to use the most common UV-based LPG inscription technique. Fortunately, there are alternative techniques. We used one of these alternative techniques, which is $CO_2$-laser inscription. Even though there are other reports on inscribing LPGs into active fibers with other alternative techniques [23,24], no optical pumping was performed in Ref. 24 and no features inaccessible by a cascade of EDF and LPG were observed in Ref. 23. This is to our opinion mainly due to the fact that the EDF used had relatively low absorption coefficient of up to 16 dB/m [23] at its peak (around 1530 nm). This corresponds to $\alpha_1 = 1.8$ $m^{-1}$, which would require very long LPGs (close to one meter) to perform the tuning [22].

To overcome this issue, we demonstrate our technique using Er80-8/125 fiber from Liekki, Finland that has 1532-nm peak absorption of 80 dB/m (corresponding to $\alpha_1 = 9.2$ $m^{-1}$) and numerical aperture comparable to standard telecom fibers (0.13). This numerical aperture leads to three advantages: low splicing loss with standard fibers, lower nonlinearities, and longer period of LPG, which enables easier LPG fabrication using techniques like $CO_2$.

First, we spliced a 15-cm piece of EDF in between two pigtails made of a standard fiber. From one side, a broadband signal combined with a pump diode (976-nm, max. power of 220 mW) through a 980/1550-nm coupler was launched. The other side of the EDF was connected into an optical spectrum analyzer. Two experiments shown demonstrate features predicted theoretically, Fig. 16, specifically the LPG tuning capability through loss/gain control and, as a special case, the feature that LPG of any strength can be tuned to the full-coupling condition. In the first demonstration, Fig.16a, the tuning capabilities are demonstrated for LPG that is close to the full-coupling condition. The other experiment, Fig. 16b, demonstrates an over-coupled LPG with the strength $\kappa L > \pi/2$ brought to the full-coupling condition by inducing appropriate gain level. The input power was set to 0.5 mW and the pump power was increased gradually from 0 to the maximum value of 220 mW, Figs. 2a and 2b. Fig. 16a clearly confirms that the resonant condition can be varied through the gain – here, the LPG dip increased from 7 dB (this would correspond to $\kappa L=0.35\pi$ for an LPG in a lossless fiber (LLF), pump of 0 mW) to the resonant value of 28 dB (corresponding to LLF-LPG $\kappa L=0.495\pi$., pump power of 32 mW) to 18 dB (corresponding to LLF-LPG $\kappa L=0.54\pi$, pump of 220 mW) while the off-resonance transmission monotonously increased at the same time from -12 dB to 3.5 dB (measured at 1531 nm). Fig. 16b shows the full-coupling condition for the LPG with $\kappa L>\pi/2$, i.e. in our case, $\kappa L=0.57\pi$ with the off-resonance amplification of 3.5 dB (measured at 1527 nm).

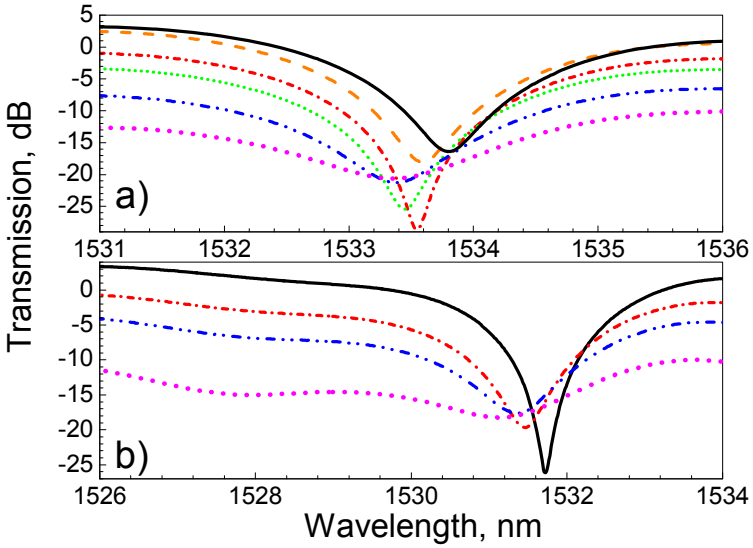


Fig. 16. Measured transmission of LPG at $\kappa L=0.52\pi$ (a) and $\kappa L=0.57\pi$ (b) for input signal of 0.5 mW and different pump power levels (0 mW, magenta short dash; 8 mW, blue dash dot dot; 17 mW, green dot; 32 mW, red dash dot; 145 mW, orange dot; 220 mW, black solid).

## 6. Summary

The presented work represents an important contribution to the field of all-optical signal processing. It focuses on 'long-term', as well as 'short-terms' goals. The long-term goals are represented by future complex all-optical signal processors that would be built from a large number of basic building blocks like logical gates, optical differentiators and integrators, etc. We addressed one of these basic building blocks, which is an all-optical differetiator. We demonstrated this device both theoretically and experimentally, having bandwidth of several THz. The short-term goals are represented by simple all-optical signal circuits that perform specific tasks. We concentrated on a synthesis of ultrashort flat-top waveforms that are of interest in ultrahigh speed optical telecommunications. In collaboration with our research partners, we successfully tested the developed devices in telecommunication systems operating at repetition rates up to 640 GHz.

## 7. Identification of the author's own contribution

The dissertation consists of the collection of articles published by the author (R. Slavík), his students and collaborators in peer-reviewed journals. All of them were written when the author was with his current employer, Institute of Photonics and Electronics AS CR, v.v.i., in which he built modern photonics laboratory that enabled the experimetnal realization and characterization of LPG filters used in the work covered by this thesis. They are numbered as A1 – A10. Although the work covered by the thesis was made since 2005, he has been working in this field since 2001. Articles reporting results of his work specifically in this field in the time period of 2002-2005 are numbered as B1- B10.

A common theme of publications covered by this thesis is ultrafast (picoseconds and sub-picoseconds) all-optical signal processing, especially using fiber-optics based filters. The author's contribution to this collaborative work was following:

1) Design of part of optical filters.
2) Fabrication, and characterization of all of fiber-optic filters used.
3) Realization of an important part of pulse shaping and signal processing experiments. The rest of experiments was made as a joint effort during the author's visits at collaborating partners.
4) Supervision of students.

## *References*

### A. Author's publications included in the thesis


[A1] R. Slavík, Y. Park, M. Kulishov, R. Morandotti, and J. Azaña, **"**Ultrafast all-optical differentiators," Opt. Express **14**, 10699-10707 (2006).

[A2] R. Slavík, **"**Extremely deep long-period fiber grating made with $CO_2$ laser," IEEE Photon. Tech. Lett. **18**, 1705-1707 (2006).

[A3] M. Kulishov, D. Krčmařík, and R. Slavík, **"**Design of terahertz-bandwidth arbitrary-order temporal differentiators based on long-period fiber gratings," Opt. Lett. **32**, 2978-2980 (2007).

[A4] Y. Park, J. Azaña, and R. Slavík, **"**Ultrafast all-optical first and higher-order differentiators based on interferometers," Opt. Lett. **32**, 710-713 (2007).

[A5] Y. Park, M. Kulishov, R. Slavik, and J. Azaña, **"**Picosecond and sub-picosecond flat-top pulse generation using uniform long-period fiber grating," Opt. Express **14**, 12671-12678 (2006).

[A6] R. Slavík, Y. Park, and J. Azaña, **"**Tunable dispersion-tolerant picosecond flat-top waveform generation using an optical differentiator," Opt. Express **15**, 6717-6726 (2007).

[A7] R. Slavík and F. Todorov, **"**Tuning of long-period fibre gratings written by CO2 laser with the resonant transmission below -45 dB," Electron. Lett. **43**, 16-18 (2007).

[A8] R. Slavík, L.K. Oxenløve, M. Galili, , H.C.H. Mulvad, Y. Park, J. Azaña, and P. Jeppesen, **"**Demultiplexing of 320 Gbit/s OTDM data using ultrashort flat-top pulses," IEEE Photon. Tech. Lett. **19**, 1855-1857 (2007).

[A9] L.K. Oxenløve, R. Slavík, M. Galili, H.C.H. Mulvad, A. T. Clausen, Y. Park, J. Azaña, and P. Jeppesen, **"**640 Gbit/s timing jitter tolerant data processing using a long-period fiber grating-based flat-top pulse shaper," accepted for IEEE J. of Sel. Topics in Quant. Electron (2008).

[A10] R. Slavík and M. Kulishov, **"**Active control of long-period fiber-grating-based filters made in erbium-doped optical fibers," Opt. Lett. **32**, 757-759 (2007).


### B. Author's publications related to the subject of the thesis


[B1] R. Slavík and S. LaRochelle, **"**Design of 10-to-40 GHz and higher pulse-rate multiplication by means of coupled Fabry-Perot resonators," Opt. Commun. **247**, 307-312 (2005).

[B2] S. Doucet, R. Slavík, and S. LaRochelle, **"**Tunable dispersion and dispersion slope compensator using novel Gires-Tournois Bragg grating coupled-cavities," IEEE Photon. Tech. Lett. **16**, 2529-2531 (2004).

[B3] R. Slavík and S. LaRochelle, **"A**ll-fiber periodic filters for DWDM using a cascade of FIR and IIR lattice filters," IEEE Photon. Tech. Lett. **16**, 497-499 (2004).

[B4] R. Slavík, S. Doucet, and S. LaRochelle, **"**High-performance all-fiber Fabry-Perot filters with superimposed chirped Bragg gratings," J. of Lightwave Technol. **21**, 1059-1065 (2003).

[B5] J. Azaña, R. Slavík, P. Kockaert, L. R. Chen, and S. LaRochelle, **"**Generation of customized ultrahigh repetition rate pulse sequences using superimposed fiber Bragg gratings," J. of Lightwave Technol. **21**, 1490-1498 (2003).

[B6] R. Slavík, S. Doucet, and S. LaRochelle, **"**Polarisation selective all-fibre Fabry-Perot filters with superimposed chirped Bragg gratings in high-birefringence fibers," Electron. Lett. **39**, 650-651 (2003).
[B7] J. Azaña, P. Kockaert, R. Slavík, L. R. Chen, and S. LaRochelle, **"**Generation of a 100-GHz optical pulse train by pulse repetition-rate multiplication using superimposed fiber Bragg gratings," IEEE Photon. Tech. Lett. **15**, 413-415 (2003).
[B8] J. Azaña, R. Slavík, P. Kockaert, L. R. Chen, and S. LaRochelle, **"**Generation of ultra-high repetition rate optical pulse bursts by means of fibre Bragg gratings operating in transmission," Electron. Lett. **38**, 1555-1556 (2002).
[B9] S. Doucet, R. Slavík, and S. LaRochelle, **"**High-finesse large band Fabry-Perot fibre filter with superimposed chirped Bragg gratings," Electron. Lett. **38**, 402-403 (2002).
[B10] R. Slavík and S. LaRochelle, **"**Large-band periodic filters for DWDM using multiple-superimposed fiber Bragg gratings," IEEE Photon. Tech. Lett. **14**, 1704-1707 (2002).

## C. Other references

[1] C. K. Madsen, D. Dragoman, and J. Azaña (editors), Special Issue on "Signal Analysis Tools for Optical Signal Processing," in EURASIP J. Appl. Signal Proc. 2005, No. 10 (2005).
[2] J. Azaña, C. K. Madsen, K. Takiguchi, and G. Cincontti (editors), Special Issue on "Optical Signal Processing," in IEEE/OSA J. Ligthwave Technol. **24**, No. 7 (2006).
[3] S. J. Kim, T. J. Eom, B. H. Lee, and C. S. Park, "Optical temporal encoding/decoding of short pulses using cascaded long-period fiber gratings," Opt. Express **11**, 3034-3040 (2003).
[4] J. H. Lee, P. C. The, P. Petropoulos, M. Ibsen, and D. J. Richardson, "All-optical modulation and demultiplexing systems with significant timing jitter tolerance through incorporation of pulse shaping fiber Bragg gratings," IEEE Photon. Technol. Lett. **14**, 203-205 (2002).
[5] Y. Park, F. Li, and J. Azaña, "Characterization and optimization of optical pulse differentiation using spectral interferometry," IEEE Photon. Technol. Lett. **18**, 1798-1800 (2006).
[6] C. Finot, B. Barviau, G. Millot, A. Guryanov, A. Sysoliatin, and S. Wabnitz, "Parabolic pulse generation with active or passive dispersion decreasing optical fibers," Opt. Express **15**, 15824-15835 (2007).
[7] C. Paré, and P. A. Bélanger, "Antisymmetric soliton in a dispersion-managed system," Opt. Commun. **168**, 103-109 (1999).
[8] M. Stratmann, T. Pagel, and F. Mitschke, "Experimental observation of temporal soliton molecules," Phys. Rev. Lett. **95**, 143902-1 – 3 (2005).
[9] M.I. Braiwish, B.L. Bachim, and T.K. Gaylord, "Prototype CO2 laser-induced long-period fiber grating variable optical attenuators and optical tunable filters," Appl. Opt. **43**, 1789-1793 (2004).
[10] G.D. VanWiggeren, T.K. Gaylord, D.D. Davis, M.I. Braiwish, E.N. Glytsis, and E. Anemogiannis, "Tuning, attenuating, and switching by controlled flexure of long-period fiber gratings," Opt. Lett. **26**, 61-63 (2001).
[11] P. Petropoulos, M. Ibsen, A. D. Ellis, and D. J. Richardson, "Rectangular pulse generation based on pulse reshaping using a superstructured fiber Bragg grating," J. Lightwave Technol. **19**, 746-752 (2001).

[12] M. Nakazawa, T. Hirooka, F. Futami, and S. Watanabe, "Ideal distortion-free transmission using optical Fourier transformation and Fourier transform-limited optical pulses," IEEE Photon. Tech. Lett. **16**, 1059-1061 (2004).
[13] N. Q. Ngo, S. F. Yu, S. C. Tjin, and C.H. Kam, "A new theoretical basis of higher-derivative optical differentiators," Opt. Commun. **230**, 115-129 (2004).
[14] M. Kulishov, and J. Azaña, "Long-period fiber gratings as ultrafast optical differentiators," Opt. Lett. **30**, 2700-2702 (2005).
[15] A. Papoulis, *The Fourier Integral and its Applications*, McGraw-Hill, New York (1987).
[16] R. Kashyap, *Fiber Bragg Gratings*, Academic Press, San Diego, (1999).
[17] A.M. Vengsarkar, P.J. Lemaire, J.B. Judkins, V. Bhatia, T. Erdogan, and J.E. Sipe, **"**Long-period fiber gratings as band-rejection filters," IEEE/OSA J. Lightwave Technol. **14**, 58-65 (1996).
[18] N. K. Berger, B. Levit, B. Fischer, M. Kulishov, D. V. Plant, and J. Azaña, "Temporal differentiation of optical signals using a phase-shifted fiber Bragg grating," Opt. Express **15**, 371-381 (2007).
[19] H. J. A. Da Silva and J.J. O'Reilly, "Optical pulse modeling with Hermite-Gaussian functions," Opt. Lett. **14**, 526-528 (1989).
[20] D. Zibar, L. K. Oxenløwe, H. C. H. Mulvad, J. Mørk, M. Galili, A.T. Clausen, and P. Jeppesen, "The Impact of Gating Timing Jitter on a 160 Gb/s Demultiplexer," *Proceedings of Optical Fiber Conference* (OFC2006), March 2006, paper OTuB2.
[21] M. Kulishov, V. Grubsky, J. Schwartz, X. Daxhelet, and D.V. Plant, "Tunable Waveguide Transmission Gratings Based on Active Gain Control," IEEE J. of Quantum Electron. **40***,* 1715-1724 (2004).
[22] M. Kulishov, X. Daxhelet, V. Grubsky, J. Schwartz, and D.V. Plant, Distinctive Behaviour of Long-Period Gratings in Amplifying Waveguides, , Optical Fiber Communication conference (OFC), paper OtuB7, Anahaim, CA, March 2005.
[23] I-B. Sonh, J.-W. Song, "Gain flattened and improved double-pass two-stage EDFA using microbending long-period fiber gratings," Opt. Commun. **236**, 141-144 (2004).
[24] G. Rego, R. Falate, J.L. Santos, H. M. Salgado, J.L. Fabris, S. L. Semjonov, and E.M. Dianov, "Arc-induced long-period gratings in aluminosilicate fibers," Opt. Lett. **30**, 2065-2067 (2005).